

西田真佐夫, 嶋田志美, 斉藤誠, 加藤道夫, 長谷川健次	C型慢性肝炎に対するインターフェロン α -2bとリバビリン併用療法におけるヘモグロビン減少に関する検討	医療薬学	30	53-58	2004
加藤道夫	くり返しTwo-step Interferon Rebound Therapyが奏功した難治性C型慢性肝炎の1例	治療学	38	73-75	2004
加藤道夫, 結城暢一, 伊与田賢也, 山本佳司, 林紀夫	Two-step interferon rebound therapyとその適応	日本臨床増刊号 ウイルス性肝炎 (上)	62	497-501	2004
伊与田賢也, 加藤道夫	C型慢性肝炎に対するIFN再治療の成績とその適応	日本臨床増刊号 ウイルス性肝炎 (上)	62	502-505	2004
結城暢一, 加藤道夫	HBV replicationのマーカーとしてのウイルス関連蛋白	日本臨床増刊号 ウイルス性肝炎 (下)	62	33-35	2004
加藤道夫	アデホビル	臨床消化器内科	20	613-620	2005
加藤道夫	B型慢性肝炎治療の最前線 インターフェロン療法	総合臨床	54	541-547	2005
金子 晃 久保光彦 渡辺晋一郎 東谷光庸 山本守敏 巽 信之 中間昭弘 尾下正秀 片山和宏 井上敦雄 春名能通 吉原治正 久保田真司 三田英治 鈴木都男 加藤道夫 脇岡泰三 萩原秀紀 平松直樹 林 紀夫	原発性胆汁性肝硬変に対するbezafibrate療法の有効性と問題点	肝臓	46	200-207	2005

加藤道夫	B型慢性肝炎の病態をどう把握し、治療方針を立てるか？	Medical Prctice	23	51-55	2006
大石和佳、茶山一彰	Lamivudine 耐性ウイルスとその治療	内科	93	491-494	2004
大石和佳、茶山一彰	非B型、非C型肝炎	Annual Review 消化器		282-286	2004;
大石和佳、茶山一彰 日本臨床増刊.	HCV-RNA 定性的測定法 (Detection of hepatitis C virus RNA)	肝炎ウイルス (上) -基礎・臨床研究の進歩-	6	214-218	2004
大石和佳、茶山一彰	B型慢性肝炎に対するラミブジン療法ーその問題点と対策ー	最新医学	59	1919-1923	2004
大石和佳、森 奈美、柘植雅貴、高木慎太郎、丁 守哲、平賀伸彦、児玉英章、平松 憲、脇 浩司、白川寛夫、相方 浩、今村道雄、高石英樹、高橋祥一、神安雅哉、茶山一彰	アーキテクトによるHBc抗体価測定 of 臨床的有用性に関する検討	肝臓	45	555-556	2004
柘植雅貴、茶山一彰	HBc抗体 (IgM-HBc抗体, IgA-HBc抗体を含む)	日本臨床増刊. 肝炎ウイルス(下)			2004
光井富貴子、茶山一彰	慢性肝炎のインターフェロン再治療	肝胆膵	49	1005-1011	2004;

今村道雄, 茶山一彰	病気のおはなし, C型肝炎	検査と技術	31	1266-1269	2004
今村道雄, 茶山一彰	C型肝炎ウイルス遺伝子からみたインターフェロン治療	治療学	38	47-50	2004
今村道雄, 茶山一彰	B型肝炎のインターフェロン療法	診断と治療	92	1872-1876	2004
今村道雄, 茶山一彰	慢性肝炎	Pharmavision		814	2004

Methylation status of suppressor of cytokine signaling-1 gene in hepatocellular carcinoma

HIDEYUKI MIYOSHI¹, HAJIME FUJIE¹, KYOJI MORIYA¹, YOSHIKAZU SHINTANI¹, TAKEYA TSUTSUMI¹, MASATOSHI MAKUUCHI², SATOSHI KIMURA¹, and KAZUHIKO KOIKE¹

¹Department of Internal Medicine, Graduate School of Medicine, University of Tokyo, 7-3-1 Hongo, Bunkyo-ku, Tokyo 113-8655, Japan

²Department of Hepatobiliary and Pancreatic Surgery, Graduate School of Medicine, University of Tokyo, Tokyo, Japan

Editorial on page 598

Background. Silencing of the suppressor of cytokine signaling (*SOCS-1*) by aberrant methylation at the CpG island in the coding region gene has been reported in hepatocellular carcinoma (HCC). However, principally, it is methylation in the 5'-noncoding region but not that in the coding region which determines the regulation of gene expression. **Methods.** Methylation-specific PCR was performed for the analysis of methylation status both in the 5'-noncoding region and the CpG island of *SOCS-1* from 22 HCC tissue samples with adjacent non-HCC tissue samples and from two cell lines. **Results.** Using primers in the CpG island, 9 of 22 HCC samples exhibited aberrant methylation of *SOCS-1*, while only 1 of 22 adjacent non-HCC samples did so. The unmethylation pattern was detected in 1 of 22 HCC and in 5 of 22 non-HCC samples. Thus, aberrant methylation of *SOCS-1* was significantly associated with HCC ($P = 0.0076$ by Fisher's exact test). Using primers in the 5'-noncoding region, aberrant methylation was observed in 12 of 22 HCC and in 2 non-HCC samples. The unmethylated pattern was observed in 5 of 22 HCC and in 10 of 22 non-HCC samples ($P = 0.0042$). There was no significant correlation between the methylation status of *SOCS-1* and clinicopathological findings, such as the presence or absence of cirrhosis or the histological grade of HCC. **Conclusions.** Aberrant methylation of the *SOCS-1* had a significant correlation with HCC. The rate of aberrant methylation was similar in the 5'-noncoding region and in the CpG island. Aberrant methylation of *SOCS-1* may be associated with hepatocarcinogenesis, although further studies are necessary.

Key words: *SOCS-1*, hepatocellular carcinoma, methylation

Introduction

The majority of cases of hepatocellular carcinoma (HCC) are associated with hepatitis B or C viral infection.^{1,2} Despite the absence of an appropriate in vitro replication system or a practical infectious animal model system, the mechanism underlying hepatocarcinogenesis in human hepatitis viral infection is on a stable path to elucidation, albeit slowly. Both the direct and indirect effects of hepatitis viruses on HCC development have been shown.³⁻⁶ Accumulation of gene aberrations, such as inactivation of tumor suppressor genes or activation of oncogenes, which may be induced through inflammation-mediated continuous death of hepatocytes followed by regeneration, is considered to be one of the mechanisms underlying hepatocarcinogenesis.^{3,4} On the other hand, viral gene products are suggested to contribute to HCC development by their direct effects on hepatocytes.⁵⁻⁸ Such direct effects have been demonstrated by the use of model systems including mice.⁵⁻⁷

In contrast, gene alterations that play pivotal roles in hepatocarcinogenesis in the majority of HCC tissues have not been identified yet. To date, the genes for the APC-axin-GSK-3 β complex may be only one of such candidate genes.^{9,10} Such gene alterations include not only mutations in the genes per se but also epigenetic changes, which lead to either suppression or augmentation of gene expression. A change in the methylation state of the gene is one of the epigenetic changes that are associated with carcinogenesis. A possible role of methylation of genes in HCC development has been reported¹¹ for a tumor suppressor gene, *p16^{INK4}*; *p16^{INK4}* expression was downregulated by methylation of the

Received: July 9, 2003 / Accepted: November 7, 2003
Reprint requests to: K. Koike

control region. Expression of some other cancer-related genes may also be inhibited by methylation.

Silencing of the suppressor of cytokine signaling-1 (*SOCS-1*; also known as *SSI-1* or *JAB*) is a member of the *SOCS* protein family. It switches off cytokine signaling by directly interacting with Janus kinase (*JAK*) proteins; its expression renders cells unresponsive to interleukin-6 stimulation.¹² The SH2 domain of *SOCS-1* binds to a JH1 domain of *JAK2* and inhibits its phosphorylation, downregulating the *JAK/STAT* pathway.^{12,13} *SOCS-1* inhibits the biological effects of cytokines *in vivo*; its forced expression interrupts macrophage differentiation induced by IL-6 and suppresses CD23 expression induced by IL-4.^{12,13} Thus, *SOCS-1* modulates the immune system through interacting with the cytokine network.

Recently, *SOCS-1*-deficient mice have been shown to die within 3 weeks after birth from a myeloproliferative disorder resulting from unbridled interferon (*IFN*)- γ and tumor necrosis factor (*TNF*)- α signaling.¹⁴ As a negative regulator of cytokine signaling, *SOCS-1* is now a candidate gene for inactivating mutations that will favor the development of malignancies; *SOCS-1* may inhibit cell proliferation induced by oncogenic forms of other known *SOCS-1*-interacting proteins. In addition to the results in hematopoietic neoplasia, recently suppression of *SOCS-1* expression has been reported in HCC, in which the CpG-rich domain in the coding region of *SOCS-1* was found to be aberrantly methylated.¹⁵ However, in general, it is the methylation of the 5' non-coding region, which contains the promoter, but not that of the coding region, which determines gene expression.^{16,17} We therefore conducted this experiment to evaluate the methylation status of the *SOCS-1* in HCC by methylation-specific PCR (*MSPCR*) using primers located both in the 5'-noncoding region and in the CpG-rich domain (CpG island) of the coding region.

Patients and methods

Patients

We studied 22 patients (19 males and 3 females; median age, 63.5 years) with HCC who had underlying chronic hepatitis C with or without cirrhosis (8 without and 14 with cirrhosis), all of whom underwent hepatectomy between 1997 and 2000 at the University of Tokyo Hospital. This study was approved by the ethics review committee of the institute, and carried out in accordance with the World Medical Association Helsinki Declaration, adopted in 1964 and amended in 1996. Informed consent was obtained from each patient. All the patients were positive for anti-hepatitis C virus (*HCV*)

confirmed by the second-generation enzyme immunoassay and *HCV*-RNA by reverse-transcriptase-polymerase chain reaction (*RT-PCR*), and none were positive for serum hepatitis B surface antigen (*HBsAg*). The clinicopathological features of the patients are shown in Table 1.

Tissue samples and cell lines

The cancerous (HCC) and noncancerous (non-HCC) liver tissue samples obtained from these patients were fixed in 10% formalin for hematoxylin and eosin staining, or immediately frozen and stored at -80°C until further use. The histological staging of the noncancerous tissues was performed according to the European classification for chronic hepatitis,¹⁸ and that of cancerous tissue was based on the TNM classification.¹⁹ All the 22 tumors were classified as advanced HCCs: 5 well-, 14 moderately, and 3 poorly differentiated HCCs (see Table 1). Human HCC cell lines *PLC/PRF/5*, *HuH-7*, and the B-cell line, *BJAB*, were obtained from the American Type Culture Collections. The cells were grown in Dulbecco's modified Eagle's medium (*DMEM*) supplemented with 10% fetal bovine serum.

DNA preparation and bisulfite treatment

Genomic DNA was extracted from the frozen tissues by standard proteinase K digestion and phenol/chloroform extraction.²⁰ Then, bisulfite modification of genomic DNA was carried out as described previously²¹ with slight modification. Briefly, DNA (1 μg) in a volume of 20 μl was denatured by NaOH at a final concentration at 0.3 M for 15 min at 37°C . Then, 113 μl 3.6 M sodium bisulfite (Sigma-Aldrich, St. Louis, MO, USA) at pH 5 and 7.2 μl 10 mM hydroquinone (Sigma-Aldrich), both freshly prepared, were added and mixed well. Then, the samples were incubated under mineral oil at 95°C for 15 min followed by incubation at 50°C for 4 h, and this cycle was repeated 15 times. Modified DNA was purified and resuspended in 50 μl water. The modification was completed by adding NaOH at a final concentration of 0.3 M for 5 min at room temperature, after which ethanol precipitation was carried out.

Genomic and methylation-specific PCR (*MSPCR*)

Bisulfite-modified and unmodified DNA was subjected to amplification using the PCR method. Primers used for the PCR in the current study are shown in Table 2. Amplification was carried out in a thermal cycler for a total of 35 cycles consisting of 95°C for 30 s, 60°C for 30 s, and 30°C for 30 s at 72°C in 50 μl reaction mixture containing 200 mM deoxynucleoside triphosphates (*dNTPs*), 1.0 mM of each primer, and $1\times$ PCR buffer [16.6 mM

Table 1. SOCS-1 gene methylation and clinicopathological findings of 22 hepatocellular carcinoma (HCC) patients

	<i>n</i>	Methylation of SOCS-1							
		CpG island				5'-noncoding			
		M ^a		U ^a		M ^a		U ^a	
		HCC	nHCC	HCC	nHCC	HCC	nHCC	HCC	nHCC
Sex									
Male	19	7	1	1	4	10	2	5	9
Female	3	2	0	0	1	2	0	0	1
Cirrhosis									
-	8	2	0	0	1	3	0	2	4
+	14	7	1	1	4	9	3	3	5
Pathology of HCC ^b									
WD	5	3	0	0	2	3	0	1	3
MD	14	4	1	1	2	7	1	3	6
PD	3	2	0	0	1	2	1	1	0
Tumor size (cm)									
<2	5	2	0	0	0	2	2	2	1
≥2	17	7	1	1	5	10	0	3	9
Vascular invasion									
Absent	19	8	1	1	4	11	2	5	9
Present	3	1	0	0	1	1	0	0	1
Distant metastasis ^c									
M0	20	9	1	1	4	12	1	4	10
M1	2	0	0	0	1	0	1	1	0
Stage grouping ^c									
I	4	1	0	0	0	1	2	2	1
II	5	3	0	0	2	3	0	1	2
III	11	4	1	0	3	6	1	2	7
IV	2	1	0	1	0	2	0	0	0
Overall	22	9*	1*	1*	5*	12*	2*	5*	10*
		(41%)	(5%)	(5%)	(23%)	(55%)	(9%)	(23%)	(46%)

^aM, hypermethylated pattern; U, unmethylated pattern; not all samples were informative for methylation status

^bWD, well-differentiated; MD, moderately differentiated; PD, poorly differentiated

^cAccording to TNM classification

**P* < 0.01 when the association of HCC and methylation was judged by Fisher's exact test for each of CpG island and 5'-noncoding region

Table 2. Polymerase chain reaction (PCR) primers used in the current study

	Sequence	Position
Forward		
HM1F	TTCGCGTGATTTTTAGGTCGGTC	(400-423)
HM2F	GAGTATTCGCGTGATTTTTAGG	(395-417)
UM1F	TTATGAGTATTTGTGTGATTTTTAGGTTGGTT	(391-423)
UM2F	TGAGTATTTGTGTGATTTTTAGG	(394-417)
UMPF-M	GTTCCGTTTCGTTTAGTTTTCGAGG	(-708-684)
UMPF-U	GTTTGGTTTTGTTTAGTTTTGAGG	(-708-684)
Reverse		
HM1R	CGACACAACCTCCTACAACGACCG	(537-559)
UM1R	CACTAACACAACACTGGTACAACAACCA	(537-565)
UM2R	CAACACAACCTCCTACAACAACCA	(543-565)
UMPR-M	ACCCCGACCGACCGCGATCTC	(-590-570)
UMPR-U	ACCCCAACCAACCACAATCTC	(-590-570)

ammonium sulfate, 67 mM Tris-HCl (pH 8.8), 6.7 mM MgCl₂, 10 mM 2-mercaptoethanol, and 0.001% (w/v) gelatin] and 1.25 units of Ampli-Taq polymerase (Perkin-Elmer Cetus, Norwalk, CT, USA). The PCR products were separated in a 2.0% agarose gel and visualized by staining with ethidium bromide.

Reverse transcription (RT)-PCR

Total RNA was extracted from cells using RNeasy (TEL-TEST, Friendswood, TX, USA). Three micrograms of total RNA were reverse transcribed by Superscript II (Gibco-BRL, Gaithersburg, MD, USA) using oligo(dT) primer and subjected to PCR. Primers for RT-PCR of *SOCS-1* gene expression were as follows: forward, 5'-CACGCACTTCCGCACATTCC-3'; reverse, 5'-TCCAGCAGCTCGAAGAGGCA-3'. For the RT-PCR, the quantity of cDNA template and the number of amplification cycles were optimized to ensure that the reaction was terminated during the linear phase of product amplification, so that semiquantitative comparisons of the mRNA abundance between different samples were possible. RT-PCR with glyceraldehyde phosphate dehydrogenase (GAPDH) primers was done to adjust the amounts of RNA in each experiment.

Statistical analysis

Fisher's exact test was used for statistical evaluation, and *P* values below 0.05 were considered significant.

Results

Methylation status of *SOCS-1* in cultured cell lines

First, the methylation status of the CpG island in the coding region of *SOCS-1* was analyzed in cell lines by MSPCR using the primer sets, HM1F+HM1R and UM1F+UM1R, according to the method of Yoshikawa et al.¹⁵ MSPCR using these primers, however, could not determine the methylation status of the gene: the use of the primers resulted in dimer formation without methylation- or unmethylation-specific bands. We therefore redesigned new sets of primers located in the CpG island of *SOCS-1* (Table 2; HM2F+HM1R for detecting a methylation-specific band and UM2F+UM2R for an unmethylation-specific band). MSPCR with these sets of primers enabled successful detection of methylation- and unmethylation-specific bands in PLC/PRF/5 cells (Fig. 1). The unmethylation-specific band alone was detected in HuH-7 cells, in agreement with the previous report.¹⁵

Analysis using the primers located in the 5'-noncoding region (see Table 2) yielded a similar pat-

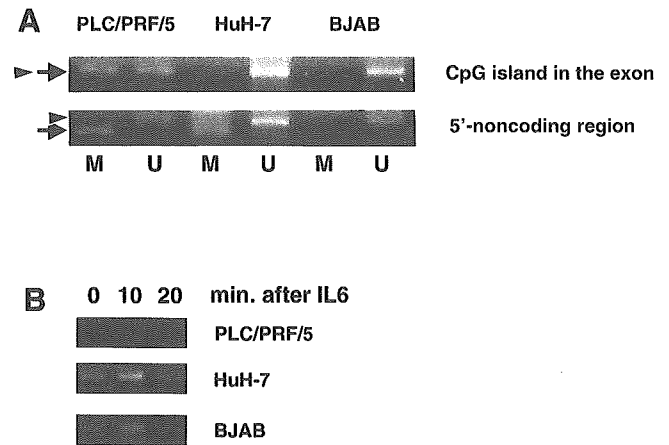


Fig. 1. Genomic and methylation-specific (MSPCR) analysis of cultured hepatoma cell lines in the CpG island and 5'-non-coding region of the *SOCS-1* gene. DNA from human hepatoma cell lines, PLC/PRF/5 and HuH-7, and a B-cell line, BJAB, was analyzed by MSPCR after bisulfite treatment as described in the Patients and methods section. **A** MSPCR with the primers in the CpG island and those in the 5'-noncoding region. **B** RT-PCR showing the expression of *SOCS-1* in cell lines before and after the addition of IL-6 (10 ng/ml). The arrow indicates the position of the methylation-specific band; the arrowhead indicates the position of the unmethylation-specific band. M, MSPCR with methylation-specific primers; U, MSPCR with unmethylation-specific primers

tern, excluding that there were both methylation- and unmethylation-specific bands also in HuH-7 cells (Fig. 1). Accordingly, the primer sets HM2F+HM1R and UM2F+UM2R were used for the analysis of the methylation status of the CpG island, and UMPF-M+UMPR-M and UMPF-U+UMPR-U were used for the 5'-noncoding region, thereafter.

Expression of *SOCS-1* mRNA in cell lines

The expression of *SOCS-1* was determined by semiquantitative RT-PCR. Although *SOCS-1* expression was abundant in HuH-7 and BJAB cells in the baseline and was enhanced by the addition of IL-6 (10 ng/ml), only marginal expression and no enhancement were detected in PLC/PRF/5 cells. These results are consistent with the methylation status that was determined in the current study and with the expression status in the baseline that was observed in a previous report.¹⁵

Methylation status of *SOCS-1* in human tumor samples

Then, DNA extracted from human HCC and non-HCC tissues was tested for the methylation status of the *SOCS-1* by MSPCR. Only 10 and 6 tissue samples were informative for determining a methylation-specific band

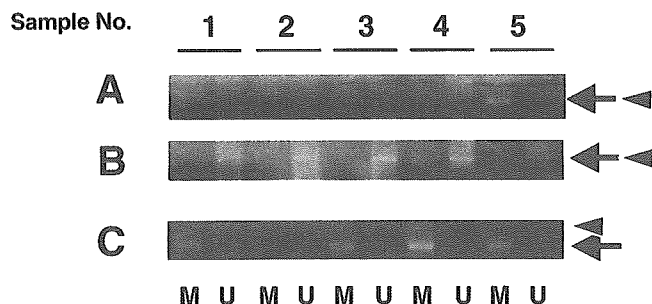


Fig. 2. MSPCR analysis of the CpG island and 5'-noncoding region of the *SOCS-1* from 22 HCC tissue samples. With the same primers used in Fig. 1, 22 pairs of HCC and non-HCC samples were analyzed by MSPCR. Representative cases are shown. Samples 1 and 2 were well-differentiated HCC, 3 and 4 were moderately differentiated HCC, and 5 was poorly differentiated HCC. Panel B shows their non-HCC counterparts. A MSPCR of DNA from HCC tissue samples with the primers in CpG island. B MSPCR of DNA from non-HCC tissue samples with the primers in CpG island. C MSPCR of DNA from HCC tissue samples with the primers in 5'-noncoding region. The arrow indicates the position of the methylation-specific band; the arrowhead indicates the position of the unmethylation-specific band HCC, hepatocellular carcinoma; M, MSPCR with methylation-specific primers; U, MSPCR with unmethylation-specific primers

and an unmethylation-specific band, respectively, when the primers in the CpG island were used. In 9 HCC tissue samples the band indicative of aberrant methylation in the CpG island was detected, while the band indicating unmethylation was detected in 1 HCC tissue sample (Fig. 2). In contrast, in the corresponding non-HCC tissue samples, only 1 exhibited the methylation pattern, whereas the unmethylation pattern was observed in 5 non-HCC tissue samples. Thus, aberrant methylation of *SOCS-1* was significantly associated with HCC rather than with non-HCC tissues ($P = 0.0076$ by Fisher's exact test).

Using primers in the 5'-noncoding promoter region, 14 and 15 HCC tissue samples were informative for a methylation-specific band and an unmethylation-specific band, respectively. Aberrant methylation was observed in 12 HCC tissue samples whereas the unmethylation pattern was detected in 5 HCC tissue samples. In contrast, only 2 non-HCC tissues exhibited aberrant methylation whereas the unmethylation pattern was detected in 10 non-HCC tissues: there was also a significant correlation between HCC and aberrant methylation of *SOCS-1* ($P = 0.0042$).

Neither a methylation-specific nor an unmethylation-specific band in 12 HCC and 16 non-HCC tissues was detected using the primers in the CpG island and in 5 HCC and 10 non-HCC tissue samples using the primers in the 5'-noncoding promoter region, suggesting that *SOCS-1* in these tissues was in a mosaic state of methylation.

This suggestion was examined using a hepatoma cell line HLF: neither a methylation- nor an unmethylation-specific band was detected, but after 5-azacytidine treatment of the cell line for 3 days, which cancels methylation of the gene,²² an unmethylation-specific band appeared, demonstrating that *SOCS-1* in the cell line is methylated in a mosaic fashion. Consequently, *SOCS-1* gene expression was turned on as determined by RT-PCR.

Correlation between SOCS-1 methylation and clinicopathological findings

The relationship between the methylation status of *SOCS-1* and clinicopathological findings is shown in Table 1. When the methylation status in HCC tissue samples was correlated with parameters such as the presence or absence of cirrhosis as the underlying liver disease, the histological degree of HCC, tumor sizes, vascular invasion, distant metastasis, or tumor stages, no significant association was noted.

Discussion

In the current study, we analyzed the methylation status of *SOCS-1*, a negative regulator of the JAK/STAT pathway, by the MSPCR method. Using the primers located in the CpG island in the coding region, aberrant methylation was observed in 9 of 22 (41%) HCC tissue samples, and 12 of 22 (54.5%) HCC tissue samples by the use of primers in the 5'-noncoding region. The former rate is almost compatible with the incidence in a previous report.¹⁴ It is notable that a similar or higher rate of aberrant methylation was detected in the 5'-noncoding promoter region of *SOCS-1*. It is established that methylation in the promoter region is essential in the regulation of (silencing) the genes.^{16,17} The frequent occurrence of aberrant methylation in the promoter region of *SOCS-1* further supports the notion that the downregulation of *SOCS-1* expression is common in human HCC. Very recently, methylation in the promoter of *SOCS-1* gene was reported in pancreatic tumors.²³

In our MSPCR analysis, a substantial number of samples showed neither the methylated nor unmethylated pattern. The reason for this dual negativity is unclear. One possibility is a mosaic methylation pattern that may exist in the *SOCS-1*. If not all the susceptible cytosine residues are methylation, i.e., a gene is methylated in a mosaic fashion, one cannot determine the methylation status by MSPCR. This possibility was confirmed using a hepatoma cell line, as shown in the Results section. Neither a methylation- nor an unmethylation-specific band was detected, but after

5-azacytidine treatment of the cell line for 3 days, which cancels methylation of the gene,²² an unmethylation-specific band appeared, demonstrating that *SOCS-1* in the cell line is methylated in a mosaic fashion.

SOCS-1 transcription is activated by signal transducer and activator of transcription (STAT) and the resultant proteins negatively regulate the JAK/STAT pathways either by directly inhibiting JAKs or by binding to receptors and blocking further association with STATs. Of the eight SOCS family members, SOCS-1 is a negative regulator of IL-6 signals. The silencing of *SOCS-1* results in constitutive activation of the JAK/STAT pathway. Without negative feedback by SOCS-1, the downstream pathways and target genes are strongly activated.²⁴ There are several lines of evidence supporting the idea that the JAK/STAT pathway may be involved in oncogenesis. The constitutive activation of the JAK/STAT pathway including STAT3 is observed in a number of transformed cells.²⁵ Thus, SOCS-1 is considered to be a tumor suppressor candidate, which chiefly has a role in the development of hematopoietic malignancies.²⁶ Also, an association of the SOCS-1 in hepatocarcinogenesis has recently been suggested.¹⁵ There are a variety of gene products in the downstream of the JAK/STAT pathway, including *c-myc* or *c-fos*.²⁷ The activation of the pathway thus may cause an activation of oncogenes or growth-associated genes and eventually lead to oncogenesis. The precise role of SOCS-1 in hepatocarcinogenesis is currently unclarified and requires further study, but it might play an essential role in the majority of HCCs.

Our current results confirmed those of a previous study¹⁴ and added a new piece of information on methylation of the promoter region of *SOCS-1*. However, the presence of cases negative for both methylation and unmethylation may limit the application of this technique for the analysis of hepatocarcinogenesis. In addition, recently the association between the core protein of hepatitis C virus and the JAK/STAT pathway has been reported as a potential proliferator of hepatocytes.²⁸ Besides aberrant methylation, association of SOCS-1 with HCV may cause a down-regulation of *SOCS-1* expression. In relation to this issue, it is interesting to note that a few patients in our series exhibited aberrant methylation of *SOCS-1* in the adjacent non-HCC tissue samples. Infection with HCV, which is present in all patients, may be associated with *SOCS-1* expression in human HCC tissues. Further studies are necessary for deciphering the complicated involvement of the SOCS-1 and JAK/STAT pathway in hepatocarcinogenesis, possibly in association with HCV infection.

References

- Chen CJ, Yu MW, Liaw YF. Epidemiological characteristics and risk factors of hepatocellular carcinoma. *J Gastroenterol Hepatol* 1997;12:S294-308.
- Saito I, Miyamura T, Ohbayashi A, Harada H, Katayama T, Kikuchi S, et al. Hepatitis C virus infection is associated with the development of hepatocellular carcinoma. *Proc Natl Acad Sci U S A* 1990;87:6547-9.
- Robinson WS. Molecular events in the pathogenesis of hepatitis B virus-associated hepatocellular carcinoma. *Annu Rev Med* 1994;45:297-323.
- Umeda T, Hino O. Molecular aspects of human hepatocarcinogenesis mediated by inflammation: from hypercarcinogenic state to normo- or hypocarcinogenic state. *Oncology* 2002;62:38-42.
- Kim CM, Koike K, Saito I, Miyamura T, Jay G. HBx gene of hepatitis B virus induces liver cancer in transgenic mice. *Nature (Lond)* 1991;351:317-20.
- Moriya K, Fujie H, Shintani Y, Yotsuyanagi H, Tsutsumi T, Matsuura Y, et al. The core protein of hepatitis C virus induces hepatocellular carcinoma in transgenic mice. *Nat Med* 1998;4:1065-7.
- Lerat H, Honda M, Beard MR, Loesch K, Sun J, Yang Y, et al. Steatosis and liver cancer in transgenic mice expressing the structural and nonstructural proteins of hepatitis C virus. *Gastroenterology* 2002;122:352-65.
- Koike K, Tsutsumi T, Fujie H, Shintani Y, Moriya K. Role of hepatitis viruses in hepatocarcinogenesis. *Oncology* 2002;62:29-37.
- Satoh S, Daigo Y, Furukawa Y, Kato T, Miwa N, Nishiwaki T, et al. AXIN1 mutations in hepatocellular carcinomas, and growth suppression in cancer cells by virus-mediated transfer of AXIN1. *Nat Genet* 2000;24:245-50.
- Fujie H, Moriya K, Shintani Y, Tsutsumi T, Takayama T, Makuuchi M, et al. Frequent β -catenin aberration in human hepatocellular carcinoma. *Hepatology* 2001;20:39-51.
- Matsuda Y, Ichida T, Matsuzawa J, Sugimura K, Asakura H. p16^{INK4} is inactivated by extensive CpG methylation in human hepatocellular carcinoma. *Gastroenterology* 1999;116:394-400.
- Starr R, Willson TA, Viney EM, Murray LJ, Rayner JR, Jenkins BJ, et al. A family of cytokine-inducible inhibitors of signaling. *Nature (Lond)* 1997;387:917-21.
- Endo TA, Masuhara M, Yokouchi M, Suzuki R, Sakamoto H, Mitsui K, et al. A new protein containing an SH2 domain that inhibits JAK kinases. *Nature* 1997;387:921-4.
- Naka T, Matsumoto T, Narazaki M, Fujimoto M, Morita Y, Ohsawa Y, et al. Accelerated apoptosis of lymphocytes by augmented induction of Bax in SSI-1 (STAT-induced STAT inhibitor-1) deficient mice. *Proc Natl Acad Sci U S A* 1998;95:15577-82.
- Yoshikawa H, Matsubara K, Qian GS, Jackson P, Groopman JD, Manning JE, et al. SOCS-1, a negative regulator of the JAK/STAT pathway, is silenced by methylation in human hepatocellular carcinoma and shows growth-suppression activity. *Nat Genet* 2001;28:29-35.
- Jaenisch R, Bird A. Epigenetic regulation of gene expression: how the genome integrates intrinsic and environmental signals. *Nat Genet* 2003;33:245-54.
- Herman JG, Baylin SB. Promoter-region hypermethylation and gene silencing in human cancer. *Curr Top Microbiol Immunol* 2000;249:35-54.
- Desmet VJ, Gerber M, Hoofnagle JH, Manns M, Scheuer PJ. Classification of chronic hepatitis: diagnosis, grading and staging. *Hepatology* 1994;19:1513-20.
- Hermanek P, Sobin LH. UICC TNM classification of malignant tumors. 4th ed. Berlin: Springer; 1987.
- Yotsuyanagi H, Yasuda K, Iino S, Moriya K, Fujie H, Shintani Y, et al. Persistent viremia after recovery from self-limited acute hepatitis B. *Hepatology* 1998;27:1377-82.

21. Herman JG, Graff JR, Myohanen S, Nelkin BD, Baylin SB. Methylation-specific PCR: a novel PCR assay for methylation status of CpG islands. *Proc Natl Acad Sci U S A* 1996;93:9821–6.
22. Velicescu M, Weisenberger DJ, Gonzales FA, Tsai YC, Nguyen CT, Jones PA. Cell division is required for de novo methylation of CpG islands in bladder cancer cells. *Cancer Res* 2002;62:2378–84.
23. House MG, Guo M, Iacobuzio-Donahue C, Herman JG. Molecular progression of promoter methylation in intraductal papillary mucinous neoplasms (IPMN) of the pancreas. *Carcinogenesis (Oxf)* 2003;24:193–8.
24. Greenhalgh CJ, Miller ME, Hilton DJ, Lund PK. Suppressors of cytokine signaling: relevance to gastrointestinal function and disease. *Gastroenterology* 2002;123:2064–81.
25. Kishimoto T, Kikutani H. Knocking the SOCS off a tumor suppressor. *Nat Genet* 2001;28:4–5.
26. Rottapel R, Ilangumaran S, Neale C, La Rose J, Ho JM, Nguyen MH, et al. The tumor suppressor activity of SOCS-1. *Oncogene* 2002;21:4351–62.
27. Darnell JE Jr, Kerr IM, Stark GR. Jak-STAT pathways and transcriptional activation in response to IFNs and other extracellular signaling proteins. *Science* 1994;264:1415–21.
28. Yoshida T, Hanada T, Tokuhisa T, Kosai K, Sata M, Kohara M, et al. Activation of STAT3 by the hepatitis C virus core protein leads to cellular transformation. *J Exp Med* 2002;196:641–53.



Serum lipid profile of patients with genotype 1b hepatitis C viral infection in Japan

Kyoji Moriya^{a,b}, Yoshizumi Shintani^a, Hajime Fujie^b, Hideyuki Miyoshi^b,
Takeya Tsutsumi^a, Hiroshi Yotsuyanagi^c, Shiro Iino^c, Satoshi Kimura^a,
Kazuhiko Koike^{a,*}

^a Department of Gastroenterology, Internal Medicine, Graduate School of Medicine, University of Tokyo, 7-3-1 Hongo, Bunkyo-ku, Tokyo 113-8655, Japan

^b Department of Gastroenterology and Hepatology, St. Marianna University School of Medicine, Kawasaki, Japan

^c Department of Infectious Diseases, Internal Medicine, Graduate School of Medicine, University of Tokyo, 7-3-1 Hongo, Bunkyo-ku, Tokyo 113-8655, Japan

Received 6 June 2002; received in revised form 7 August 2002; accepted 24 October 2002

Abstract

Hepatitis C virus (HCV) infection is associated with the development of steatosis in the liver. Recently, infection with genotype 3a HCV has been reported to have a closer association with hepatic steatosis than that with genotype 1 or 2 HCV. Moreover, infection with genotype 3a HCV but not with genotype 1 has been shown to be associated with serum hypocholesterolemia or hypobetalipoproteinemia in European countries. We conducted a case control study to characterize the serum lipid profile in patients infected with genotype 1b HCV, which is the most prevalent HCV genotype in Japan. These patients had significantly lower serum cholesterol levels than those infected with HBV or genotype 2a HCV who had similar liver disease progression and body mass index. Further analysis of serum apolipoproteins revealed that not only apolipoprotein B but also apolipoprotein CII and apolipoprotein CIII levels were significantly reduced, while apolipoprotein AI, AII and E levels were similar in patients infected with genotype 1b HCV and those with HBV or genotype 2a HCV. These results indicate that, in Japan, infection with genotype 1b HCV is a cause of lipid metabolism disturbances, which may be associated with the pathogenesis of hepatitis C liver disease. © 2002 Elsevier Science B.V. All rights reserved.

Keywords: Apolipoprotein; Hypocholesterolemia; Steatosis

1. Introduction

Infection with hepatitis C virus (HCV) is the cause of a sequence of liver diseases that finally leads to the development of hepatocellular carcinoma (HCC) worldwide [1,2]. Chronic hepatitis C, which precedes the development of HCC, is

* Corresponding author. Tel.: +81-3-5800-8801; fax: +81-3-5800-8807.

E-mail address: kkoike-tky@umin.ac.jp (K. Koike).

characterized by several histopathologic features: lymphocytic follicle formation, bile duct damage and steatosis (fatty change) [3–5]. In addition, an association between HCV infection and lipid metabolism has been extensively reported. For example, the low-density-lipoprotein (LDL) receptor [6,7] is suggested to be associated with HCV particles, and analysis using a cell culture system has revealed that the secretion of apolipoprotein AII from cells is modulated by the core protein of HCV [8,9]. In experimental animal models, the core protein or nonstructural protein(s) of HCV is steatogenic when expressed in the liver of mice [10,11]. Lipid analysis of fatty liver in mice transgenic for the HCV core gene revealed that the amount of carbon 18 mono-unsaturated fatty acids increased, being distinct from lipid accumulation in the fatty liver of simple obesity mice [12]. Importantly, those transgenic mouse strains develop HCC after the phase of hepatic steatosis [11,13]. Therefore, it is essential to elucidate the changes in lipid metabolism in patients with HCV infection.

Recently, several reports from European countries have pointed out that the degrees of hepatic steatosis are different among chronic hepatitis C patients depending on the genotype of the infecting virus: steatosis is more marked in patients with genotype 3a HCV infection, which is moderately prevalent in European countries such as France or Italy [14] than in those with genotype 1 or 2 infection [15–17]. In addition, hypocholesterolemia or hypobetalipoproteinemia was observed only in patients with genotype 3a HCV infection but not in those with genotype 1 HCV infection [17]. However, in Japan where the genotype 3 HCV infection is very rare, hepatic steatosis is also common in patients with chronic hepatitis of genotype 1b HCV infection, and the detection of the HCV core protein in liver tissue is an independent risk factor for steatosis in a specific liver tissue by multivariate analysis [18,19]. We, therefore, explored for dyslipidemia or alteration in lipid metabolism in patients with genotype 1b HCV infection in Japan by determining the levels of lipids and apolipoproteins in the serum.

2. Patients and methods

2.1. Patients

We studied 50 patients (male:female = 30:20) with histologically proven noncirrhotic chronic hepatitis C who were admitted to our hospitals from January 1999 to December 2000. Patients were selected according to the following criteria: (1) presence of HCV-RNA in serum; (2) absence of cirrhosis; (3) a body mass index (BMI) < 25; (4) alcohol consumption < 40 g/day; (5) absence of evident diabetes; and (6) not taking drugs influencing lipid metabolism (lipid-lowering agents, non-steroidal anti-inflammatory drugs (NSAIDs)). Exclusion of cirrhotic patients was done by limiting the patients to only those who showed F1 or F2 [3,4] on liver biopsy that was performed within 1 year before serum lipid determination. Diagnosis of overt diabetes was done according to the guidelines of Japan Diabetes Society: at least two determinations of fasting blood glucose \geq 126 mg/dl or casual blood glucose \geq 200 mg/dl. Patients were regarded not to have overt diabetes if they did not meet this criterion and were not subject to insulin or oral hypoglycemic agents. The general characteristics of the 50 patients are shown in Table 1. All the patients were negative for the hepatitis B surface antigen (HBsAg) in serum. Informed consent was obtained from the patients, and human experimentation guidelines of the hospitals were followed in the conduct of this research.

As a control, 50 patients infected with hepatitis B virus (HBV) were selected according to the same criteria for selection of hepatitis C patients except for the criterion (1). Instead, the presence of HBsAg and absence of HCV-RNA in serum have been added as a criterion.

2.2. Viral serology

The levels of HBsAg, antibody to HBsAg (anti-HBs) and anti-HCV in the sera were determined using commercially available enzyme immunoassay kits (Dainabot, Tokyo, Japan) according to the manufacturer's instructions. HCV-RNA levels were determined using a commercially available

Table 1
Comparison of patients with chronic hepatitis C (C-CH) and chronic hepatitis B (B-CH)

	C-CH (N = 50)	B-CH (N = 50)	P
Age (years)	57.3±9.0	55.2±11.4	0.257
Sex	30:20	30:20	–
BMI (kg/m ²)	22.4±2.9	21.9±2.9	0.434
ALT (IU/l)	50.1±40.6	57.3±70.7	0.534
Albumin (g/dl)	4.21±0.21	4.16±0.20	0.282
Prothrombin time (%)	90.2±11.9	89.8±11.6	0.859
Total cholesterol (mg/dl)	167.4±37.7	195.6±38.3	<0.0005*
HDL-cholesterol (mg/dl)	55.2±16.7	59.7±17.6	0.277
Triglyceride (mg/dl)	122.8±63.6	129.8±67.5	0.637
Apolipoprotein AI (mg/dl)	134.5±20.1	140.2±29.5	0.263
Apolipoprotein AII (mg/dl)	28.8±5.9	28.5±6.4	0.787
Apolipoprotein B (mg/dl)	78.1±21.3	105.8±24.4	<0.0001*
Apolipoprotein CII (mg/dl)	2.15±1.35	3.98±1.87	<0.0001*
Apolipoprotein CIII (mg/dl)	6.74±2.17	8.87±2.60	<0.0001*
Apolipoprotein E (mg/dl)	4.17±1.08	4.31±0.95	0.618
Serum HCV-RNA (KIU/ml)	245±200		
HCV genotype 1b	40		
2a	10		

*Statistically significant.

kit (Amplicor HCV monitor v2.0, Roche Diagnostic Systems, Branchburg, NJ). The genotype of HCV was determined by RT-PCR with primers in the core region as described previously [20].

2.3. Laboratory investigations

Levels of total and HDL cholesterol, triglycerides and other biochemical parameters including apolipoproteins measured in the serum or plasma were using an auto-analyzer (Hitachi 7600 auto-analyzer, Tokyo, Japan). All assays were performed using fresh serum samples drawn from patients after at least 12 h fasting without taking alcohol overnight.

2.4. Statistical analysis

Results are expressed as means±S.E. The significance of the difference of means was determined using Student's *t*-test. Differences are considered significant when $P < 0.05$.

3. Results

Serum apolipoprotein levels and other parameters were determined; serum samples were drawn from patients infected with HCV and those with HBV (control) after at least 12 h of fasting. As shown in Table 1, there was no significant difference in age, sex ratio or BMI between the patients infected with HCV and those with HBV. Moreover, there was no difference in liver function between the two groups as assessed by alanine aminotransferase (ALT) or albumin level or prothrombin time level. Total cholesterol, and apolipoproteins B, CII and CIII levels were significantly lower in patients infected with HCV than those with HBV, while there was no significant difference in the levels of apolipoprotein AI, AII or E between these two groups (Table 1). Thus, there was dyslipidemia in patients with HCV infection, although there was no significant difference in the synthesis function of the liver between the two groups. There was no significant difference in serum lipid profile between the patients with histological degrees of F1 and F2, although the number of patients with F1 was small.

By analysis of the HCV genotype, 40 of the 50 chronic hepatitis C patients were found to have genotype 1b HCV, while the remaining ten patients had genotype 2a HCV. There were no patients with genotype 2b or other genotypes. These results are compatible with the prevalence of HCV genotypes in Japan as reported previously, where the prevalence of genotype 1b is about 70%, genotype 2a about 25% and genotype 2b about 5% [21,22]. There was no significant difference in age, sex ratio, BMI, serum albumin level, prothrombin time, platelet count or serum HCV-RNA level between the patients infected with genotype 1b HCV and those with genotype 2a HCV. Total cholesterol, and apolipoproteins B,

CII and CIII levels were significantly lower in patients infected with genotype 1b HCV than those with genotype 2a HCV, while there was no significant difference in the level of apolipoprotein AI, AII or E between the two groups (Table 2). There was no significant difference in the levels of apolipoproteins between the patients infected with genotype 2a HCV and those infected with HBV. There was no significant correlation between the levels of HCV-RNA and lipid profiles in patients with genotype 1b HCV infection. However, it might be possible that analysis of a larger number of patients leads to a significant correlation.

4. Discussion

Disturbance in lipid metabolism in HCV infection has been suggested by several lines of evidence: (1) steatosis in the liver of hepatitis C patients [3–5], (2) steatosis in the liver of transgenic mice harboring the HCV core gene or the entire HCV genome [10,11], (3) a possible role of LDL receptors in HCV entry into cells [6,7] and (4) association between the HCV core protein and apolipoprotein AII in an experimental system [8,9]. In addition, hypocholesterolemia has recently been documented in HCV infection and

suggested as a possible basis for steatosis [17]. Interestingly, these reports from European countries stated that only HCV of genotype 3a is associated with hepatic steatosis or hypocholesterolemia, while HCV of genotype 1, 2 or 4 is scarcely associated with lipid metabolism disturbance, particularly with dyslipidemia [15–17]. However, the association of hepatic steatosis with HCV infection has also been documented in Japan, where about 70% of HCV infection was of genotype 1b [21,22]. In addition, HCV constructs used in the experimental steatosis mouse models are of genotype 1b from Japanese patients [10,11]. Therefore, it is of a great importance to assess whether chronic hepatitis C with genotype 1b HCV in Japan has an abnormality in lipid metabolism represented by dyslipidemia.

Our current results clearly indicate that patients with HCV infection in Japan have disturbances in lipid metabolism compared with those with HBV infection, and the disorder is attributed not to genotype 2a but to genotype 1b HCV infection, although the number of patients with genotype 2a HCV may be small. In our cohort, this is not due to other common causes of dyslipidemia, such as malignancy, poor liver function, intestinal malabsorption or inherited disorders of lipids. Indeed, cirrhotic patients were excluded, and patients with

Table 2
Comparison of patients with hepatitis C virus of genotype 1b and genotype 2a

	Genotype 1b (N = 40)	Genotype 2a (N = 10)	P
Age (years)	57.6 ± 6.1	56.1 ± 5.9	0.493
Sex	24:16	6:4	–
BMI (kg/m ²)	22.4 ± 3.0	22.1 ± 2.2	0.694
Albumin (g/dl)	4.23 ± 0.21	4.12 ± 0.21	0.142
Platelet count (× 10 ⁴ /μl)	17.6 ± 5.0	16.8 ± 3.1	0.658
PT (%)	90.0 ± 12.4	93.6 ± 8.5	0.386
Total cholesterol (mg/dl)	159.0 ± 27.4	211.9 ± 44.4	< 0.0001*
HDL-cholesterol (mg/dl)	53.4 ± 13.5	60.6 ± 24.7	0.297
Triglyceride (mg/dl)	121.5 ± 66.0	128.4 ± 55.5	0.788
Apolipoprotein A I (mg/dl)	133.8 ± 20.0	137.1 ± 21.3	0.636
Apolipoprotein AII (mg/dl)	28.6 ± 5.9	29.8 ± 6.0	0.541
Apolipoprotein B (mg/dl)	76.3 ± 15.7	89.7 ± 26.8	0.039*
Apolipoprotein CII (mg/dl)	1.86 ± 0.92	3.18 ± 2.04	0.003*
Apolipoprotein CIII (mg/dl)	6.35 ± 1.40	8.09 ± 3.62	0.018*
Apolipoprotein E (mg/dl)	4.07 ± 0.88	4.49 ± 1.58	0.383
Serum HCV-RNA (KIU/ml)	247 ± 199	234 ± 218	0.868

*Statistically significant.

or without dyslipidemia were not significantly different in terms of prothrombin time or serum albumin level. It is not clear whether or not genotype 3a HCV is more closely associated with disturbances in lipid metabolism than genotype 1b in Japan, because there are very few, if any, patients with genotype 3a HCV infection in Japan [21,22].

It is of an interest that not only apolipoprotein B but also apolipoprotein CII and CIII levels were low in patients with genotype 1b HCV infection in Japan, whereas apolipoprotein AI, AII and E levels were similar to those in control groups. Because apolipoprotein CII and CIII are present in both high-density lipoprotein (HDL) and very-low density lipoprotein (VLDL), and apolipoprotein B is present in VLDL and LDL, impairment of synthesis or secretion of VLDL in the liver may explain these observations. In a mouse model of hepatic steatosis that is transgenic for the HCV core gene, secretion of VLDL from the liver is disrupted chiefly due to the decrease in the level of the microsomal triglyceride transfer protein [23]. Moreover, it might be interesting to know that peroxisome proliferator-activated receptor- α (PPAR- α) activates the transcription of *apolipoprotein AI* and *AII* genes and suppresses the *apolipoprotein CII* and *CIII* genes in humans [24,25]. In fact, association of the HCV core protein with PPAR- α has been observed in an experimental system (Tanaka N, Moriya K, Kamijo Y, Kiyosawa K, Koike K, Aoyama T., unpublished data). Further studies are necessary to clarify the mechanism underlying lipid disturbance in HCV infection.

It is unclear at present why there is a difference in observations for genotype 1b HCV, which may induce lipid metabolism disturbances, between Japan and European countries. It may be noteworthy that determining the amino acid sequences of nonstructural region 5A of genotype 1b HCV genome is useful for the prediction of IFN responsiveness of patients in Japan but is not effective in studies from European countries [26,27]. Thus, there may be some differences in amino acid sequences, which are responsible for the development of distinct features of hepatitis C including hepatic steatosis, in the genotype 1b

HCV clones between Japan and European countries. Further studies are required to elucidate the 'steatogenic' region in the HCV genome.

References

- [1] Saito I, Miyamura T, Ohbayashi A, et al. Hepatitis C virus infection is associated with the development of hepatocellular carcinoma. *Proc Natl Acad Sci USA* 1990;87:6547–9.
- [2] Simonetti RG, Camma C, Fiorello F, et al. Hepatitis C virus infection as a risk factor for hepatocellular carcinoma in patients with cirrhosis. *Ann Intern Med* 1992;116:97–102.
- [3] Bach N, Thung SN, Schaffner F. The histological features of chronic hepatitis C and autoimmune chronic hepatitis: a comparative analysis. *Hepatology* 1992;15:572–7.
- [4] Lefkowitz JH, Schiff ER, Davis GL, et al. Pathological diagnosis of chronic hepatitis C: a multicenter comparative study with chronic hepatitis B. *Gastroenterology* 1993;104:595–603.
- [5] Scheuer PJ, Ashrafzadeh P, Sherlock S, Brown D, Dusheiko GM. The pathology of chronic hepatitis C. *Hepatology* 1992;15:567–71.
- [6] Agnello V, Abel G, Elfahal M, Knight GB, Zhang QX. Hepatitis C virus and other flaviviridae viruses enter cells via low-density lipoprotein receptor. *Proc Natl Acad Sci USA* 1996;96:12766–71.
- [7] Monazahian M, Bohme I, Bonk S, et al. Low density lipoprotein receptor as a candidate receptor for hepatitis C virus. *J Med Virol* 1999;57:223–9.
- [8] Barba G, Harper F, Harada T, et al. Hepatitis C virus core protein shows a cytoplasmic localization and associates to cellular lipid storage droplet. *Proc Natl Acad Sci USA* 1997;94:1200–5.
- [9] Sabile A, Perlemuter G, Bono F, et al. Hepatitis C virus core protein binds to apolipoprotein AII and its secretion is modulated by fibrates. *Hepatology* 1999;30:1064–76.
- [10] Moriya K, Yotsuyanagi H, Shintani Y, Fujie H, Ishibashi K, Matsuura Y, et al. Hepatitis C virus core protein induces hepatic steatosis in transgenic mice. *J Gen Virol* 1997;78:1527–31.
- [11] Lerat H, Honda M, Beard MR, et al. Steatosis and liver cancer in transgenic mice expressing the structural and nonstructural proteins of hepatitis C virus. *Gastroenterology* 2002;122:352–65.
- [12] Moriya K, Todoroki T, Tsutsumi T, et al. Increase of carbon 18 mono-unsaturated fatty acids in the liver of hepatitis C: Analysis in transgenic mice and humans. *Biophys Biochem Res Commun* 2001;281:1207–12.
- [13] Moriya K, Fujie H, Shintani Y, et al. Hepatitis C virus core protein induces hepatocellular carcinoma in transgenic mice. *Nature Med* 1998;4:1065–8.
- [14] Pawlotsky JM, Tsakiris L, Roudot-Thoraval F, et al. Relationship between hepatitis C virus genotypes and

- sources of infection in patients with chronic hepatitis C. *J Infect Dis* 1999;171:1607–10.
- [15] Rubbia-Brandt L, Quadri R, Abid K, et al. Hepatocyte steatosis is a cytopathic effect of hepatitis C virus genotype 3. *J Hepatol* 2000;33:106–15.
- [16] Mihm S, Fayyazi A, Hartmann H, Ramadori G. Analysis of histopathological manifestations of chronic hepatitis C virus infection with respect to virus genotype. *Hepatology* 1997;25:735–9.
- [17] Serfaty L, Andreani T, Giral P, Carbonell N, Chazouilleres O, Poupon R. Hepatitis C virus induced hypobetalipoproteinemia: a possible mechanism for steatosis in chronic hepatitis C. *J Hepatol* 2001;34:428–34.
- [18] Fujie H, Yotsuyanagi H, Moriya K, et al. Steatosis and intrahepatic hepatitis C virus in chronic hepatitis. *J Med Virol* 1999;59:141–5.
- [19] Haruna Y, Miyamoto T, Yasunami R, Kanda T, Fushimi H, Kotoh K. Human leukocyte antigen DRB1 1302 protects against bile duct damage and portal lymphocyte infiltration in patients with chronic hepatitis C. *J Hepatol* 2000;32:837–42.
- [20] Yotsuyanagi H, Koike K, Yasuda K, et al. Hepatitis C virus genotypes and development of hepatocellular carcinoma. *Cancer* 1995;76:1352–5.
- [21] Okamoto H, Mishiro S. Genetic heterogeneity of hepatitis C virus. *Intervirology* 1994;37:68–76.
- [22] Ohno O, Mizokami M, Wu RR, et al. New hepatitis C virus (HCV) genotyping system that allows for identification of HCV genotypes 1a, 1b, 2a, 2b, 3a, 3b, 4, 5a, and 6a. *J Clin Microbiol* 1997;35:201–7.
- [23] Perlemuter G, Sabile A, Letteron P, et al. Hepatitis C virus core protein inhibits triglyceride-transfer protein activity and very low-density lipoprotein secretion: a model of viral-related steatosis. *FASEB J* 2002;16:185–94.
- [24] Vu-Dac N, Schoonjans K, Laine B, Fruchart JC, Auwerx J, Staels B. Negative regulation of the human apolipoprotein A-I promoter by fibrates can be attenuated by the interaction of the peroxisome proliferator-activated receptor with its response element. *J Biol Chem* 1994;269:31012–8.
- [25] Vu-Dac N, Schoonjans K, Kosykh V, et al. Fibrates increase human apolipoprotein A-II expression through activation of the peroxisome proliferator-activated receptor. *J Clin Invest* 1995;96:741–50.
- [26] Enomoto N, Sakuma I, Asahina Y, et al. Mutations in the nonstructural protein 5A gene and response to interferon in patients with chronic hepatitis C virus 1b infection. *New Eng J Med* 1996;334:77–81.
- [27] Brechot C. The direct interplay between HCV NS5A protein and interferon transduction signal: from clinical to basic science. *J Hepatol* 1999;30:1152–4.

BASIC-LIVER, PANCREAS, AND BILIARY TRACT

Hepatitis C Virus Infection and Diabetes: Direct Involvement of the Virus in the Development of Insulin Resistance

YOSHIZUMI SHINTANI,* HAJIME FUJIE,* HIDEYUKI MIYOSHI,* TAKEYA TSUTSUMI,*
KAZUHISA TSUKAMOTO,† SATOSHI KIMURA,* KYOJI MORIYA,* and KAZUHIKO KOIKE*

Departments of *Internal Medicine and †Metabolic Diseases, Graduate School of Medicine, University of Tokyo, Tokyo, Japan

See editorial on page 917.

Background & Aims: Epidemiological studies have suggested a linkage between type 2 diabetes and chronic hepatitis C virus (HCV) infection. However, the presence of additional factors such as obesity, aging, or cirrhosis prevents the establishment of a definite relationship between these 2 conditions. **Methods:** A mouse model transgenic for the HCV core gene was used. **Results:** In the glucose tolerance test, plasma glucose levels were higher at all time points including in the fasting state in the core gene transgenic mice than in control mice, although the difference was not statistically significant. In contrast, the transgenic mice exhibited a marked insulin resistance as revealed by the insulin tolerance test, as well as significantly higher basal serum insulin levels. Feeding with a high-fat diet led to the development of overt diabetes in the transgenic mice but not in control mice. A high level of tumor necrosis factor- α , which has been also observed in human chronic hepatitis C patients, was considered to be one of the bases of insulin resistance in the transgenic mice, which acts by disturbing tyrosine phosphorylation of insulin receptor substrate-1. Moreover, administration of an anti-tumor necrosis factor- α antibody restored insulin sensitivity. **Conclusions:** The ability of insulin to lower the plasma glucose level in the HCV transgenic mice was impaired, as observed in chronic hepatitis C patients. These results provide a direct experimental evidence for the contribution of HCV in the development of insulin resistance in human HCV infection, which finally leads to the development of type 2 diabetes.

Approximately 200 million people are chronically infected with hepatitis C virus (HCV) in the world. Chronic HCV infection may lead to cirrhosis and hepatocellular carcinoma, thereby being a worldwide problem both in medical and socioeconomic aspects.^{1,2} In addition, chronic HCV infection is a multifaceted disease, which is associated with numerous clinical manifesta-

tions, such as essential mixed cryoglobulinemia, porphyria cutanea tarda, and membranoproliferative glomerulonephritis.³ Recent epidemiological studies have added another clinical condition, type 2 diabetes, to a spectrum of HCV-associated diseases.⁴⁻⁷ However, the establishment of a definite causative relationship between HCV infection and diabetes is hampered by the presence of other factors such as obesity, aging, or liver injury in patients with chronic HCV infection.

Type 2 diabetes is a complex, multisystem disease with a pathophysiology that includes a defect in insulin secretion, increased hepatic glucose production, and resistance to the action of insulin, all of which contribute to the development of overt hyperglycemia.^{8,9} Although the precise mechanisms whereby these factors interact to produce glucose intolerance and diabetes are uncertain, it has been suggested that the final common pathway responsible for the development of type 2 diabetes is the failure of the pancreatic β -cells to compensate for the insulin resistance. Hyperinsulinemia in the fasting state is observed relatively early in type 2 diabetes, but it is considered to be a secondary response that compensates for the insulin resistance.^{8,9} Overt diabetes occurs over time when pancreatic β -cells bearing the burden of increased insulin secretion fail to compensate for the insulin resistance.

In this study, to elucidate the role of HCV in a possible association between diabetes and HCV infection, transgenic mice that carry the core gene of HCV^{10,11} were analyzed. We found that these mice developed insulin resistance. An addition of a high-calorie diet led to the development of type 2 diabetes by dis-

Abbreviations used in this paper: EDL, extensor digitorum longus; ELISA, enzyme-linked immunosorbent assay; FPG, fasting plasma glucose; HCV, hepatitis C virus; IRS, insulin receptor substrate; JNK, c-Jun N-terminal kinase; TNF- α , tumor necrosis factor- α .

© 2004 by the American Gastroenterological Association
0016-5085/04/\$30.00

doi:10.1053/j.gastro.2003.11.056

rupting the balance between insulin resistance and secretion.

Materials and Methods

Transgenic Mice

The production of HCV core gene transgenic mice has been described previously.¹¹ Briefly, the core gene from HCV of genotype 1b, which is placed downstream of a transcriptional regulatory region from the hepatitis B virus, was introduced into C57BL/6 mouse embryos (Clea Japan, Tokyo, Japan). The mice were cared for according to institutional guidelines, fed an ordinary chow diet (Funabashi Farms, Funabashi, Japan), and maintained in a specific pathogen-free state. At an indicated time, the mice were fed a high-fat diet (Oriental Yeast Co., Ltd., Tokyo, Japan) for up to 2 months. Caloric content of food was 4.70 kcal/g for high-fat diet and 3.56 kcal/g for ordinary diet. The high-fat diet contains 18.5% protein, 22.1% fat (4.7% vegetable fat and 17.4% animal fat), 5.4% ash, 2.5% fiber, 6.5% moisture, and 45.0% carbohydrate, and the ordinary diet contains 22.4% protein, 5.7% fat, 6.6% ash, 3.1% fiber, 7.7% moisture, and 54.5% carbohydrate. Because there is a sex preference in the development of liver lesion in the transgenic mice, we used only male mice that were heterozygously transgenic for the core gene, and as controls we used nontransgenic litter mates of the transgenic mice. Transgenic mice carrying the HCV envelope genes under the same regulatory region as that in the core gene transgenic mice were also used as controls.¹² At least 5 mice were used in each experiment and the data were subjected to statistical analysis.

Glucose Tolerance Test

The mice were fasted for >16 hours before the study. D-Glucose (1g/kg body weight) was administered by intraperitoneally (IP) injection to conscious mice. Blood was drawn at different time points from the orbital sinus, and plasma glucose concentrations were measured by using an automatic biochemical analyzer DRI-CHEM 3000V (Fuji Film, Tokyo, Japan). The levels of serum insulin were determined by radioimmunoassay (BIOTRAK; Amersham Pharmacia Biotech, Piscataway, NJ) with rat insulin as a standard.

Insulin Tolerance Test

The mice were fed freely and then fasted during the study period. Human insulin (1 U/kg body weight) (Humulin; Novo Nordisk, Denmark) was administered by IP injection to fasted conscious mice, and glucose concentrations were determined at the time points indicated. Values were normalized to the baseline glucose concentration at the administration of insulin.

Morphometric Analysis

Sections of the pancreas were prepared and evaluated for morphometry after H&E staining or immunostaining. Rel-

ative islet area and islet number were determined with an image analyzer (QUE-2; Olympus Optical Co., Tokyo, Japan).

Enzyme-Linked Immunosorbent Assay

ELISA for mouse tumor necrosis factor (TNF)- α was performed using a commercially available mouse TNF- α ELISA kit (BioSource International, Camarillo, CA). Samples were prepared as reported previously.¹³ Briefly, the liver of transgenic and control mice were lysed with a buffer containing 1% Tween 80, 10 mmol/L Tris-HCl [pH 7.4], 1 mmol/L EDTA, 0.05% sodium azide, 2 mmol/L PMSF, and the Protease Inhibitor Cocktail (Complete; Roche Molecular Biochemicals, Indianapolis, IN) and homogenized on ice for 20 seconds. The homogenates were centrifuged at $11,000 \times g$ for 10 minutes at 4°C, and the supernatants were collected and assayed. ELISA was performed in triplicate for each sample. The concentrations of the cytokines in the liver were normalized by determining the amount of total protein in each sample using the BCA Protein Assay Kit (Pierce, Rockford, IL).

Immunoprecipitation and Western Blotting

For immunoprecipitation studies, liver tissues were homogenized in lysis buffer (10 mmol/L Tris-HCl at pH 7.5, 150 mmol/L NaCl, 10 mmol/L sodium pyrophosphate, 1.0 mmol/L β -glycerophosphate, 1.0 mmol/L sodium orthovanadate [Na_3VO_4], 50 mmol/L sodium fluoride [NaF], the Protease Inhibitor Cocktail [Complete, Roche Molecular Biochemicals], and 1.0% Triton X-100), and homogenates were precipitated with an anti-insulin receptor substrate (IRS)-1 or anti-IRS-2 rabbit polyclonal antibody (UBI, Lake Placid, NY) and then with Sepharose 4B beads (Amersham Biosciences). Resulting pellets were washed 3 times and then subjected to Western blotting. Pellets were resuspended in Western sample buffer (5% β -mercaptoethanol, 2% sodium dodecyl sulfate, 62.5 mmol/L Tris-HCl, 1 mmol/L EDTA, 10% glycerol), and then subjected to 2%–15% gradient sodium dodecyl sulfate/PAGE (PAG Mini "DAIICHI" 2/15 (13W), Daiichi Diagnostics, Tokyo, Japan), and electrotransferred to polyvinylidene difluoride membranes (Immobilon-P, Millipore, Bedford, MA). The filter was then reacted with antiphosphorylated tyrosine (Santa Cruz Biotechnology Inc., Santa Cruz, CA), antiphosphorylated serine (Cell Signaling Technology, Inc., Beverly, MA), anti-IRS-1 or anti-IRS-2 mouse monoclonal antibody (BD Biosciences, Lexington, KY), followed by immunostaining with secondary biotinylated IgG (Vector Labs, Inc., Burlingame, CA) and visualization using an ECL kit (Amersham Intl., Buckinghamshire, UK).¹⁴

Hyperinsulinemic-Euglycemic Clamp

Mice underwent a hyperinsulinemic-euglycemic clamp using D-[3-³H]glucose (NEN Life Science, Boston, MA) to measure the rate of glucose appearance and hepatic glucose production (HGP) as described previously.¹⁵ Three days after jugular catheter placement, a hyperinsulinemic-euglycemic clamp was conducted with a continuous infusion of human

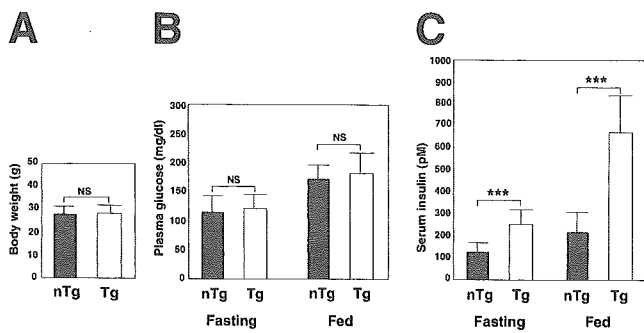


Figure 1. Altered glucose homeostasis in hepatitis C virus core gene transgenic mice. (A) Body weight of 2-month-old mice ($n = 10$ in each group). (B) Plasma glucose levels in fasting or fed mice ($n = 10$ in each group). (C) Serum insulin levels in fasting or fed mice ($n = 10$ in each group). The insulin level was significantly higher in the core gene transgenic mice than in control mice. Values are mean \pm standard error; *** $P < 0.001$; NS, statistically not significant; nTg, nontransgenic mice; Tg, transgenic mice.

insulin to raise serum insulin within a physiological range. Blood samples were drawn at intervals for the immediate measurement of blood glucose concentration, and 20% glucose was infused at variable rates to maintain blood glucose at ca. 125 mg/dL. All infusions were done using microdialysis pumps (KD Scientific Inc., Boston, MA). The rate of glucose appearance (mg/kg per minute), which equals the rate of total body glucose utilization during steady state, was calculated as the ratio of the rate of infusion of [$3\text{-}^3\text{H}$]glucose and the steady state plasma [^3H]glucose specific activity. HGP (mg/kg/min) during clamps was determined by subtracting the glucose infusion rate from the rate of glucose appearance.

Glucose Uptake by Skeletal Muscle

The extensor digitorum longus (EDL) or soleus muscle was excised from 2-month-old mice and exposed to insulin at the indicated concentrations. 2-Deoxyglucose uptake was determined as described previously.¹⁶

Treatment With Anti-TNF- α Antibody

To suppress TNF- α , a dose of 200 $\mu\text{g}/\text{mouse}$ of neutralizing hamster monoclonal antibody (TN3-19.12, Santa Cruz Biotechnology Inc.) was administered by IP injection on days 1 and 4, and plasma glucose and insulin levels were determined at day 5.¹⁷

Statistical Analysis

The results are expressed as means \pm standard error. The significance of the difference in means was determined by Student t test or Mann-Whitney U test whenever appropriate. $P < 0.05$ was considered significant.

Results

Hyperinsulinemia and Insulin Resistance in Transgenic Mice

At the age between 1 and 12 months, there was no significant difference in body weight between the core

gene transgenic mice and control mice. Figure 1A shows body weight of 2-month-old mice. Fasting plasma glucose (FPG) levels were slightly elevated in the core gene transgenic mice compared with control mice, but the difference was not significant ($P = 0.79$, Figure 1B). In contrast, there was a marked increase in the level of serum insulin in the core gene transgenic mice than control mice ($P < 0.001$, Figure 1C). Hyperinsulinemia was observed in the core gene transgenic mice as early as 1 month old. These findings suggest that decreased responsiveness to the hormone may have resulted in compensatory hyperinsulinemia. Administration of glucose to 2-month-old core gene transgenic mice revealed mild glucose intolerance compared with control mice of the same age, but the difference was not statistically significant at any time points measured (Figure 2A). HCV envelope gene transgenic mice of the same age, in which the envelope genes were expressed under the same transcriptional regulatory region as the core gene transgenic mice, did not manifest hyperinsulinemia or elevated FPG levels, indicating that not the transcriptional regulatory region used but the expressed gene itself is essential in this phenotype.

The insulin tolerance test conducted at the age of 2 months revealed that the reduction in plasma glucose concentration after IP insulin injection was impaired in the core gene transgenic mice, displaying higher plasma glucose levels than those in control mice at all time points measured (Figure 2B). At 40 and 60 minutes, the difference was statistically significant between transgenic

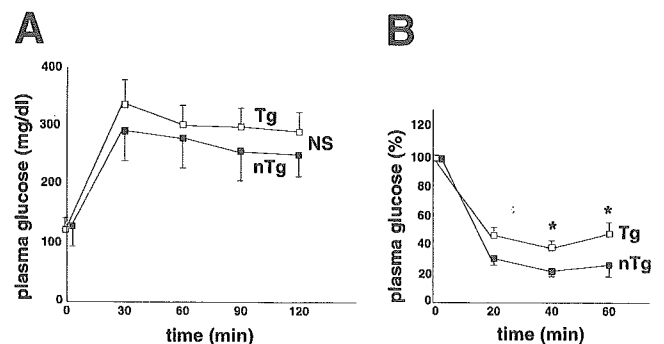


Figure 2. Insulin resistance in the core gene transgenic mice. (A) Glucose tolerance test ($n = 5$ in each group). Animals were fasted overnight (>16 hours). D-Glucose (1 g/kg body weight) was administered by IP injection to conscious mice, and plasma glucose levels were determined at the time points indicated. (B) Insulin tolerance test ($n = 5$ in each group). Human insulin (1 U/kg body weight) was administered by IP injection to fasted conscious mice and glucose concentrations were determined. Values were normalized to the baseline glucose concentration at the time of insulin administration. Values are mean \pm standard error; * $P < 0.05$; NS, statistically not significant; nTg, nontransgenic mice; Tg, transgenic mice.

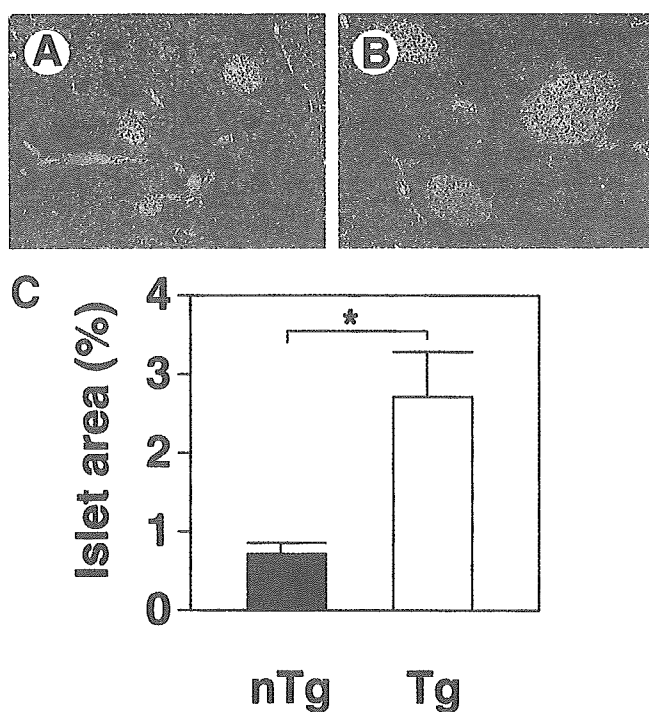


Figure 3. Analysis of pancreatic islet mass in the core gene transgenic and control mice. (A and B) Morphology of representative islets (H&E staining) from normal control mice (A) or the core gene transgenic mice (B). (C) Relative islet area, expressed as a percentage of the total stained pancreatic section, for control mice (nTg) and the core gene transgenic mice (Tg) (n = 10 in each group). Values are mean ± standard error; *P < 0.05.

and control mice (39.6 ± 1.3 vs. 24.4 ± 1.1 and 43.7 ± 2.1 vs. 26.4 ± 2.3, P < 0.05). These data are consistent with a defect in the actions of insulin on glucose disposal and/or production in the core gene transgenic mice.

Morphology of Pancreatic Islet Cells

Because a critical factor contributing to whether insulin resistance progresses to diabetes is the capacity of the pancreatic β-cells to respond to increased demands for insulin secretion, we evaluated the morphology of pancreatic islet cells by histologic examination. In the pancreas of HCV core gene transgenic mice, an approximately 3-fold increase in islet mass was observed (Figure 3, P < 0.05), which is consistent with β-cell compensation to insulin resistance. There was no infiltration of inflammatory cells within or surrounding the islets.

Feeding Transgenic Mice a High-Fat Diet Leads to Overt Diabetes

Thus, an insulin resistance is present but no apparent glucose intolerance (overt diabetes) in the HCV core gene transgenic mice. This is probably because of the genetic background of C57BL/6 mice, which has

been shown to maintain either normal or mildly elevated glucose levels despite insulin resistance.¹⁸ To determine whether a high-fat diet exacerbates the prediabetic phenotype, 2-month-old HCV core gene transgenic mice were fed a high-fat diet for up to 8 weeks. Both the transgenic and control mice showed a similar increase (about 30%) in body weight (Figure 4A). After 8 weeks on this diet, 100% (10 out of 10) of the transgenic mice exhibited casual (fed) plasma glucose levels >250 mg/dL, whereas none of the 10 control mice fed the same diet exhibited levels >250 mg/dL (325.0 ± 66.6 vs. 179.0 ± 17.4 mg/dL, P < 0.01, Figure 4B). Insulin levels were significantly higher in the core gene transgenic mice than in control mice both at fasting and fed state (Figure 4C, P < 0.01 and P < 0.001). In control mice, serum insulin levels in high-fat diet state were significantly higher than those in normal diet state at fed state (Figures 1C and 4C, P < 0.01). Although FPG levels were not significantly different between the transgenic and control mice, these results indicate that feeding a high-fat diet leads to the development of overt diabetes in a mouse model for HCV infection. Body weight gain, particularly with high levels of lipid, may trigger the process leading to overt diabetes in an insulin resistance model mouse with compensatory hyperplasia of islet cells.

Insulin Resistance in the Core Gene Transgenic Mice Is Chiefly Caused by Hepatic Insulin Resistance

We then investigated the mechanism of insulin resistance in the core gene transgenic mice. There was no

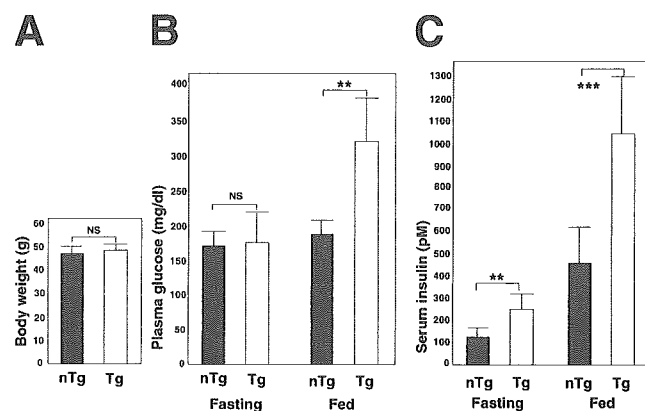


Figure 4. Body weight and glucose homeostasis after a high-fat diet. Control and transgenic mice were fed a high-fat diet for 8 weeks; thereafter, body weight and blood parameters were determined. (A) Body weight at the end of the high-fat diet (n = 10 in each group). (B) Plasma glucose levels determined in a fasting or fed state (n = 10 in each group). (C) Serum insulin levels in a fasting or fed state (n = 10 in each group). Values are mean ± standard error; NS, statistically not significant; **P < 0.01; ***P < 0.001; nTg, nontransgenic mice; Tg, transgenic mice.